SIN-CHN SCIENTIFIC PRESS PTE.LTD.

Molecular & Cellular Biomechanics 2024, 21(2), 508.
https://doi.org/10.62617/mcb.v21i2.508

Article

Medical image recognition based on multilayer neural network

Nan Ma[1,*], Yaxin Hou[2]

[1] Journal of Shanxi Politics and Law Institute for Administrations, Taiyuan 030027, China
[2] Department of Diagnostic Ultrasound, Beijing Tongren Hospital, Capital Medical University, Beijing 100730, China
*** Corresponding author:** Nan Ma, 18603516071@163.com

CITATION

Ma N, Hou Y. Medical image recognition based on multilayer neural network. Molecular & Cellular Biomechanics. 2024; 21(2): 508. https://doi.org/10.62617/mcb.v21i2.508

ARTICLE INFO

Received: 11 October 2024
Accepted: 17 October 2024
Available online: 5 November 2024

Abstract: As a common accidental injury, accurate identification of burns and scalded injuries is of great significance to the development of treatment programs and prognosis assessment. Traditional identification methods are subjective and inaccurate, this paper proposes a burns and scalds grade identification technique based on multilayer neural network. The three-degree classification standard of burns and scalds is described, and the structure and principle of multilayer neural network are introduced, including the network structure composed of input layer, hidden layer and output layer, forward propagation, back propagation and training process. The implementation steps of burns and scald grade recognition technology based on multi-layer neural network are discussed in detail, such as data acquisition, image pre-processing, feature extraction, classifier design, model training and evaluation. Through experiments, the model is tested using a dataset containing 362 burns and scalds images, and the model achieves more than 90% accuracy on the test set with high accuracy and reliability. The multi-layer neural network model is used to classify the burn and scald data, which improves the diagnostic accuracy, shortens the delay time of the disease, reduces the pressure of professional doctors, and helps patients have a preliminary understanding of the degree of burn.

Keywords: multilayer neural network; image recognition; grade prediction

1. Introduction

With the continuous development of medical technology, medical image data shows explosive growth. Medical image recognition plays a crucial role in modern medical treatment, which can assist doctors in diagnosis and improve diagnostic accuracy and efficiency [1]. Traditional medical image recognition methods are mainly based on manually extracted features, which are limited by the experience and domain knowledge of the feature designer and difficult to handle complex medical image data [2]. In contrast, medical image recognition technology based on multi-branch networks has a strong advantage in that it can automatically learn the feature representations in the data and handle complex medical image data, which brings new opportunities for medical image recognition.

In Chinese medicine, burns were first called “water and fire burns, fire burns, soup and fire burns”, which refers to burns caused by burning materials and scorching liquids, solids, gases, and electric currents that act directly on the human body, resulting in burns or scalds on the skin, and the severity of which is determined by the area of injury and the depth of burns, and serious burns not only cause great pain to patients, but also may lead to disability or even life-threatening [3,4]. Therefore, accurate identification of the grade of burns is essential for the development of rational treatment plans and assessment of prognosis. The traditional method of identifying the

grade of burns mainly relies on the clinical experience and visual observation of doctors, which is highly subjective and inaccurate [5]. Arbab et al. [6] and others used the knowledge of spectroscopy to diagnose burn wounds, but the accuracy rate was not high, which was far from meeting the requirements of intelligent diagnosis. He.ec et al. Used convolutional neural network to predict the degree of burn in the burn and scald area, trained the convolutional neural network model using the images marked by professionals, and evaluated the burn depth of the burn and scald medical image, with an average accuracy of about 80% [7]. Some people also use cameras to collect burn data and use the method of deep learning to classify burns and scalds, achieving an accuracy rate of 85% [8]. The diagnosis of burn and scald plays an important role in the follow-up treatment. If the burn and scald area cannot be treated in time, it will affect the healing time and the state of the skin in the healing area, and the patients cannot get the best treatment [9].

Deep learning algorithms can utilize known data to predict unknown data, and in the case of insufficient data, ImageNet pre-training model under the Keras framework can be utilized to classify burns data by migration learning of burn grade [8]. As a deep learning algorithm, multi-layer neural network has good feature extraction and classification ability, and has achieved remarkable results in the fields of image recognition and speech recognition [9]. In this paper, multi-layer neural network is applied to burns grade recognition to realize the accurate judgment of burns grade by feature extraction and classification of burns images.

2. Classification network model

2.1. Transfer learning

Transfer learning is manifested in human behavior as a learning mechanism of learning by touch, and in the field of computer science as a process of deepening learning on top of existing learning outcomes [10]. This process aims to recognize the correlation between new input data and previous training data, and thus evaluate the new input data. When new knowledge points need to be evaluated, we can utilize the previous learning to classify the knowledge points using the existing knowledge, and this application process is known as migration [11,12]. In the field of image processing, given that there are certain commonalities between natural images and medical images, migration can be performed using models that have been trained and matured on natural images to solve problems in medical image analysis.

Migration learning can be categorized into four types of sample-based, feature-based, model-based, and relation-based migration depending on the learning method. This study focuses on the category of feature migration and uses the pre-trained model weights on ImageNet as the basis for migration learning for burn recognition [13,14]. The process does not require a large amount of new image data, but rather the pre-trained weights are transferred to a newly constructed model based on an existing image dataset, and the model is trained twice. This method aims to utilize features common to images to ensure superior experimental results on new datasets. As for relation-based transfer learning, knowledge transfer is achieved by mapping logical relations to the target domain through the learning of relations between concepts in the source domain.

This study focuses on the migratory application of parameter sharing, and in view of the quantitative deficiencies of burns and scalds medical images compared to other types of images, the migration learning strategy is adopted to accelerate the convergence speed of the neural network model and achieve superior classification performance.

2.2. ResNet model

As a representative model in the field of deep learning, ResNet shows significant advantages in image processing tasks, especially in image classification. The network structure is similar to a series of filters. By introducing residual units, it effectively solves the problems of gradient disappearance and performance degradation caused by the increase of network depth, thus leading the new trend of feature extraction technology in the field of image recognition [15]. ResNet is built in a double-layer neuron structure. Its working principle is as follows: the input data is first processed by convolution operation and activation function, and then output the result. The result is then transmitted as the input data of the next layer. The whole process can be expressed by Equation (1):

$$a^{i+1} = g\left(W^i a^i + b^i\right) \tag{1}$$

In the L layer, W^i represents the weight matrix, and b represents the offset term. Through the action of activation function g, the output data of layer L, i.e., a^{i+2}, can be derived, and its calculation method is consistent with the above formula. In the residual network structure, the initial input features will be reused in subsequent operations, so as to realize the reuse of surface features. This process can be represented by Equations (2) and (3):

$$z^{i+2} = W^{i+2} a^i + b^i \tag{2}$$

$$a^{i+2} = g\left(z^{i+2} + a^i\right) \tag{3}$$

In the residual network architecture, the expression Z^{i+2} represents the output after convolution processing at layer l+1. Different from the activation output of the traditional convolution layer, the output of this layer is obtained by adding the convolution result of the current layer to the data of the previous layer, and then processing the activation function. This process is helpful for the network to capture the shallow data characteristics, which makes the network optimization process more smooth and easy to converge. Further increasing the depth of the network can improve its feature expression ability to a certain extent, making it more powerful [16]. The ResNet architecture used in this study is shown in **Figure 1**. Firstly, the burn image is preprocessed to construct the data set required for network training, and then the data is input into the network to train the overall model. The parameters of the model are optimized by the validation set, and the performance of the model is evaluated by the test set. Taking ResNet-50 as an example, the network contains multiple hierarchies, including convolution layer (conv), maximum pool layer (max pool), identity mapping layer (identity) and global AVG pool layer (global avg-pool). Each convolution module is composed of a convolution layer, a jump connection, batch normalization

(BN) and activation function. The core contribution of ResNet network is the introduction of jump connection technology, which solves the gradient disappearance problem in deep network training by constructing residual blocks in the hidden layer. This residual block structure is used by many subsequent algorithms.

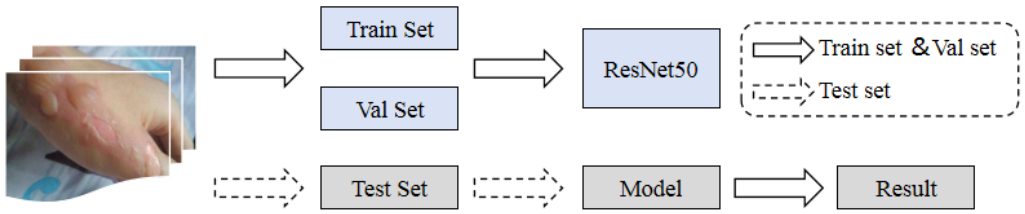

Figure 1. ResNet-50 model framework diagram.

2.3. DenseNet model

With the increase of the number of neural network layers, the conversion path from input to output is extended, which may lead to the disappearance of gradient in the process of back propagation. Both DenseNet core concept and ResNet architecture are designed to optimize network performance through the reuse of features, although they differ in the mechanism of feature reuse. The connection built by DenseNet, called concatenate, realizes the close connection between each layer and all the previous layers, that is, the input of the current layer will be the input of all subsequent layers, and each layer will fully mine features through channel connection [17]. This kind of connection mode ensures the effective transmission of the gradient when the network deepens. This process can be expressed by Equation (4):

$$X_L = H_L X_{L-1} + X_{L-1} \tag{4}$$

In the deep learning model, the symbol X_L is used to represent the output of layer L, and accordingly, X_{L-1} represents the input of layer $L-1$. H_L represents the compound function operation performed by layer L. The input of this layer is generated by accumulating the output of the previous layer. In contrast, the connection strategy adopted by DenseNet network is the concatenate operation in each channel dimension, and its structure is shown in **Figure 2**. The meanings of different colors in the figure are the same as those described above. Such connection can be expressed by Equation (5):

$$X_L = H_L(X_0, X_1, \ldots, X_{L-1}) \tag{5}$$

In the DenseNet network architecture, the fusion of the outputs of each layer is realized by the Concatenate operation, which is significantly different from the traditional convolutional neural network in terms of feature output. While traditional convolutional neural networks usually output only the highest level of features, DenseNet networks integrate different levels of feature information with the help of the Concatenate operation, which covers all the data, thus showing superior performance in the case of limited data [18]. The DenseNet architecture is mainly composed of two core components: the Dense layer and the Transition layer. In the Dense layer, the connection pattern between inputs and outputs is clarified, while the Transition layer is responsible for the efficient transfer of features by adjusting the

number of channels. Since the size of the feature maps between different layers in the Dense layer should be consistent, the feature maps are internally integrated through the Concatenate operation [19]. For feature integration between different Dense layers, instead of using Concatenate, the Transition layer is utilized for feature dimension compression, i.e., features are output through the combination of a series of convolutional and pooling layers. The network structure of DenseNet is illustrated in **Figure 2**. The image input is first passed through a convolutional layer with a step size of 2 and a convolutional kernel size of 7 × 7, followed by maximum pooling. Feature extraction and image dimensionality reduction is achieved by alternating the Dense layer with the Transition layer, and finally, processed by a global average pooling layer and a fully connected layer in order to arrive at the classification results [20].

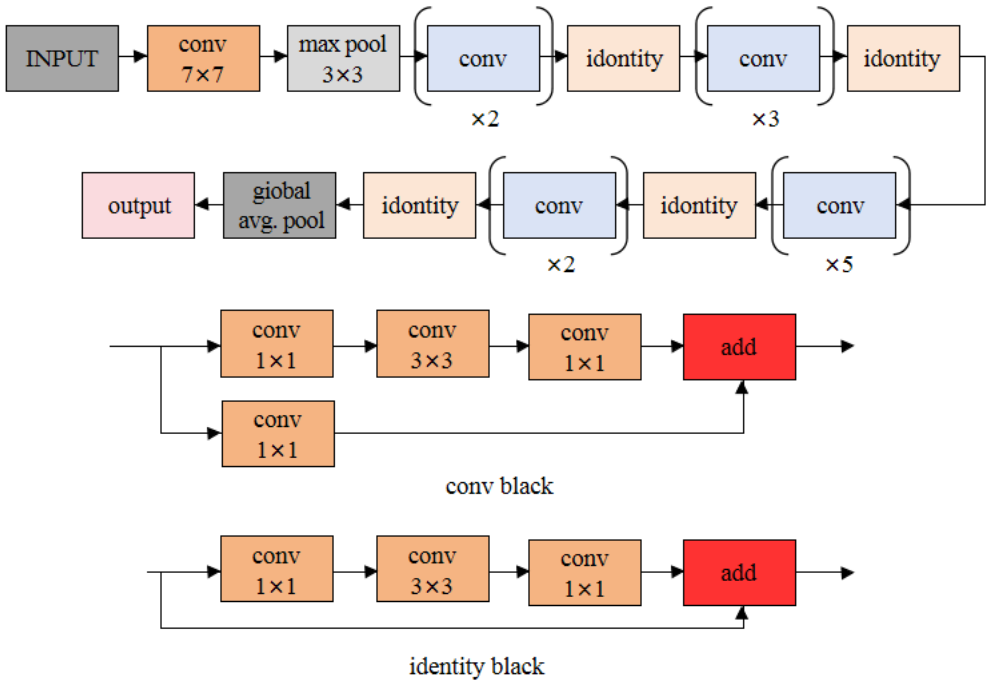

Figure 2. The network structure of DenseNet.

The number of network layers can be changed by adjusting the *k*1, *k*2, *k*3, and *k*4 parameters, and the parameter configurations of DenseNet-121, DenseNet-169, and DenseNet-201 are detailed in **Table 1**. Taking DenseNet-121 as an example, the numbering indicates that the initial stage of the network contains a 7 × 7 convolutional layer, and the subsequent four Dense layers each have (6 + 12 + 24 + 16) × 2 convolutional units, three Transition layers containing three 1 × 1 convolutional unit, and a fully connected layer for classification at the end. Compared with other network structures, DenseNet achieves a relative reduction in the total number of parameters while deepening the number of network layers, its generalization ability is stronger, it is less prone to overfitting, and the underlying features are fully utilized. In the classification task, the model is easier to train by acquiring richer information.

Table 1. DenseNet parameter table.

	DenseNet-121	DenseNet-169	DenseNet-201
$k1$	6	6	6
$k2$	12	12	12
$k3$	24	32	48
$k4$	16	32	32

3. Experimental design and analysis

3.1. Experimental environment

The classified experimental environment of this study is shown in **Table 2**. The purpose of the experiment is to classify the burn depth according to the actual situation of patients' burn treatment, including shallow burn, moderate burn and deep burn. In view of the uneven distribution of the number of burn patients and the small overall number, the collection of burn images is more challenging than other types of images, resulting in the limited size of the data set constructed. At present, there is no public burn image data set on the Internet. The data used in this study are all from burn cases in Beijing Tongren hospital in the past five years. By collecting the early wound photos of burn patients, an exclusive data set is constructed.

Table 2. Classified experimental environment.

Hardware environment	CPU: e5-2680
	GPU
	Memory: 2.5T
Software environment	Operating system: Ubuntu 16.04.5
	Language: python 2.8.0
	Environmental dependencies: Tensorflow, keras, pytorch, opencv

3.2. Inclusion and exclusion criteria

Inclusion criteria: (1) the study object should be the wound image taken within 48 hours after the occurrence of burn, and the patient must belong to the total area of burn not more than 10%; (2) When screening images, images taken from different perspectives of the same burn patient can be selected, but the number of patient images should be controlled within the range of 1 to 3, and the photos with clear local wound should be the first choice; (3) The collected photos were randomly encoded.

Exclusion criteria: (1) photos of patients with major underlying diseases or over 80 years old; (2) There are many pollutants attached to the wound, obvious drug staining, or the surface is uneven and reflective due to the application of colorless plaster; (3) Photos with less than 20KB and insufficient definition.

3.3. Classification of burn and scald levels

Mild burn: also known as erythematous burn and scald, the injury only affects the epidermal layer. The local manifestations were redness and pain of the skin without blisters. Generally, it can heal itself in 3–5 days without leaving scars.

Moderate burns: burns and deep dermis, with local swelling, small or flat blisters, and dull sensation. If there is no infection, it can be healed in 3–4 weeks, often with scar formation.

Deep burn: also known as eschar burn, the injury involves the whole skin and subcutaneous tissues, muscles, bones, etc. The local manifestations are pale, sallow or charred skin, no pain, and the feeling disappears. Wound repair depends on skin grafting or skin flap transplantation. Scar formation and dysfunction often occur after healing.

3.4. Dataset creation

After excluding patients with other severe underlying diseases, this study collected a series of wound images of burn patients. These images were divided into three categories according to the severity of injury: mild group, moderate group and depth group. In order to reduce external interference, 2–3 experts in the field of burns are specially invited to use image scope software to accurately delineate the burn area in the image in advance [21]. Subsequently, these outlined areas are processed into 224 * 224-pixel image fragments (patches), and these image fragments are randomly translated (translate along the *x*-axis and *y*-axis with *x*0 and *Y*0 coordinates in the upper left corner), rotated (rotate 60 °, 90 °, 180 ° and 270 ° counterclockwise around the center of the image) and other image enhancement operations with the help of Python program. The data set is divided into training set, verification set and test set according to the ratio of 7:1.5:1.5.

According to the established criteria, a total of 362 images of early burn wounds were screened out in this study, as shown in **Figure 3**. According to the actual healing cycle of the wound, burn experts manually marked and trimmed these images, and finally formed 4216 224 * 224 pixel wound images, including 1296 shallow burn images, 1349 moderate burn images and 1571 severe burn images, in the actual operation, the oversampling method is adopted to copy the samples in a few data, reaching the same number as the deep burn. Finally, 15,700 images for training and 3400 images for verification and testing were generated.

Figure 3. Example of burn level.

In the stage of building the network model, the specific configuration of each network parameter is listed in **Table 3**:

Table 3. Classification network parameter table.

Parameter	Definition	Value
Size	Input size	224
Epoch	Training rounds	300
Batch	Batch size	32
Optimizer	Optimizer	Adam
Loss	Loss function	BCELoss
Lr	Learning rate	1.00×10^{-4}

3.5. Evaluation criteria

The evaluation criteria of this experiment are F1_score, sensitivity (SE) and specificity (SP) [22]. We use TP, FN, FP, TN to represent true positive, false negative, false positive, true negative. The highly sensitive model can detect the potential epidemic risk in time, and the highly specific model can reduce the risk of misdiagnosis. F1_score takes into account the accuracy rate and recall rate, avoiding the deviation caused by focusing on only one of the indicators. The three can evaluate the accuracy of the network model from different angles, and provide reliable support for medical diagnosis and treatment. When we calculate F1_score, we use p (precision) and R (recall). F1_score measures both *P* and *r*.

$$P = \frac{TP}{TP + FP} \tag{6}$$

$$\text{R=TP/(TP+FN)} \tag{7}$$

$$F1\_score = \frac{2}{\frac{1}{F} + \frac{1}{R}} = \frac{2P \times R}{P + R} = \frac{2TP}{2TP + FP + FN} \tag{8}$$

$$SE = \frac{TP}{TP + FN} \tag{9}$$

$$SP = \frac{TN}{TN + FP} \tag{10}$$

The accuracy rate is the ratio of the number of records used for correct segmentation to the total number of records. F1_score measures P and R at the same time. Through the evaluation of these indicators, we can judge whether the new classification model can have a good classification effect on fewer burn and scald images.

4. Experimental results and analysis

This study focuses on three different levels of classification for the degree of burns. Based on the measured metrics, this paper calculates key parameters such as precision, recall, and F1-score to evaluate the classification performance. In this study, the Inception module was initially used as the basis for feature extraction to construct a new type of classification network, and the relevant data were derived according to the evaluation criteria. Observing the data shown in **Table 4**, it can be seen that the

accuracy of the constructed classifier in the classification of mild and moderate burns is about 68.5%, while the overall model accuracy is about 0.70, which is comparable to that of conventional manual recognition of burn grades.

Table 4. Inception-3 classification results.

Category	Precision	Recall	F1-score
Mild	0.68	0.66	0.67
Medium	0.69	0.63	0.65
Deep	0.72	0.82	0.77

As shown in **Table 5**, this study used the ResNet-50 model for feature extraction, and the recognition accuracies of all three burn classification networks exceeded 80%. Among the classification networks, the recognition performance of deep burns performed better, followed by mild burns, while the classification accuracy of medium burns was relatively low.

Table 5. ResNet-50 classification results.

Category	Precision	Recall	F1-score
Mild	0.84	0.73	0.78
Medium	0.81	0.81	0.81
Deep	0.82	0.93	0.87

In the final stage of this study, DenseNet-121 was chosen as the feature extraction tool to carry out the classification experiments. Observing the data in **Table 6**, it can be seen that DenseNet-121 presents a slight performance advantage over ResNet-50, indicating that the DenseNet architecture has a better performance in feature extraction and is able to capture the intrinsic patterns of the image more effectively. The overall accuracy of the experiment rises to approximately 0.87, achieving a significant improvement compared to the aforementioned model. Based on this, this study further explores whether enhancement in classification performance can be achieved by deepening the network structure. The network models of DenseNet-169 and DenseNet-201 were constructed, and their results are displayed in **Tables 7** and **8**, respectively. The experimental data show that with the increase of network depth, the classification effect is not significantly improved, which indicates that there are also limitations in the feature extraction ability of dense networks. This is because the network structure of densenet-121 is relatively simple, and it is easier to converge in the training process. In contrast, densenet-169 and densenet-201 have deeper network depth and greater optimization difficulty, requiring longer training time and more complex optimization strategies to achieve better performance. In actual training, if the training time is limited or the optimization strategy is not perfect, densenet-169 and densenet-201 may not be able to give full play to their performance advantages, while densenet-121 can achieve better convergence effect in a short time.

Table 6. DenseNet-121 classification results.

Category	Precision	Recall	F1-score
Mild	0.85	0.84	0.84
Medium	0.84	0.86	0.83
Deep	0.92	0.93	0.91

Table 7. DenseNet-169 classification results.

Category	Precision	Recall	F1-score
Mild	0.86	0.85	0.85
Medium	0.85	0.89	0.87
Deep	0.94	0.87	0.93

Table 8. DenseNet-201 classification results.

Category	Precision	Recall	F1-score
Mild	0.85	0.87	0.87
Medium	0.87	0.88	0.87
Deep	0.94	0.91	0.92

As shown in **Figure 4**, the scald with blisters should be classified as medium burn, but it was classified as mild burn in actual recognition, probably because the scald did not appear swelling and redness, and the color difference was small. Throughout the experiment, recognition accuracy was consistently higher for deep burns than for the other two burn types. Physicians in the study noted that deep burns were better recognized than the other burn types, which is consistent with the experimental data. This phenomenon side by side verifies that the greater the color difference, the better the classification results.

Figure 4. Example image of recognition error.

5. Discussion

In the current rapid development of computer technology, deep learning algorithms have made remarkable achievements in many fields. Especially in the field of medical image analysis, the application of deep learning technology is increasingly widespread. This study is dedicated to exploring the application of deep neural networks in the early diagnosis of burn grading, aiming to improve the accuracy of

existing deep learning-based medical image recognition techniques. The novel model constructed by using a migration learning strategy demonstrates excellent performance in the classification of burn grades, with an accuracy no less than that of medical professionals. The model is capable of rapidly recognizing burn patients' injuries, and has significant innovative and practical application potential. In addition, performing standardized processing on the data to ensure the consistent size of the images inputted into the network helps reduce the interference of the variation of the images themselves, promotes the rapid convergence of the network, and excludes the interference of other image factors on the judgment, thus improving the accuracy of the model in determining the degree of burns.

In this study, a multilayer neural network model was used to classify burn data into grades, and its accuracy, precision and efficiency were better than those of professional doctors. Judgment can be made simply by taking pictures of the same size as the model specifications and inputting them into the network model. This approach greatly reduces the time of delay in the condition of patients with acute burns, reduces the pressure on the demand for physicians specializing in burn medicine, and also enables patients to have a certain degree of awareness of the degree of burns after the first burn. In the future research, we need to design a more refined feature extractor to extract features. With the demand of applying the deep learning model to terminal devices, we need to design a more lightweight network to meet the demand. In the future, classification and classification can be combined together and image processing can be carried out at the same time. The research content can be truly applied in hospitals, and research and industry can be combined to truly realize auxiliary diagnosis.

Author contributions: Conceptualization, NM and YH; methodology, YH; software, NM; validation, NM, YH; formal analysis, NM; investigation, NM; resources, YH; data curation, YH; writing—original draft preparation, NM; writing—review and editing, NM; visualization, YH; supervision, NM; project administration, NM; funding acquisition, NM. All authors have read and agreed to the published version of the manuscript.

Fundings: This work was sponsored in part by Special Research Project on High-Quality Development of the Big Health Industry by the Shanxi Provincial Federation of Social Sciences (DJKZXKT2023081).

Ethical approval: Not applicable.

Conflict of interest: The authors declare no conflict of interest.

References

1. Tekerek A, Al-Rawe I. A Novel Approach for prediction of lung disease using chest X-ray images based on DenseNet and MobileNet. Wireless Personal Communications, 2023: 1-15.
2. Choudhury S K, Padhy R P, Sa P K. Faster R-CNN with densenet for scale aware pedestrian detection vis-à-vis hard negative suppression. IEEE, 2017.
3. Nosanov L B, Travis T E, Shawn T, et al. 586 Graft loss: 5-year review of a single burn center's experience with an institutional grading scale. Journal of Burn Care & Research, 2022, (Supplement_1): Supplement_1.
4. Suvarna M, Kumar S, Niranjan U C. Classification methods of skin burn images. international journal of computer science &

information technology, 2013.
5. Mashreky S R, Rahman A, Chowdhury S M, et al. Perceptions of rural people about childhood burns and their prevention: A basis for developing a childhood burn prevention programme in Bangladesh. Public Health, 2009, 123(8): 568-572.
6. Arbab M H, Henry S C, Warsen A, et al. Diagnosis of burn wounds using terahertz time-domain spectroscopy. IEEE, 2016.
7. Wang Y, Ke Z, He Z, et al. Real-time burn depth assessment using artificial network: a large-scale, multicentre study[J]. Burns, 2020, 46(8).
8. Romano Y, Elad M, Milanfar P. RED-UCATION: A Novel CNN Architecture Based on Denoising Nonlinearities[C]// 2018: 6762-6766.
9. Boissin C, Laflamme L, Wallis L, et al. Photograph-based diagnosis of burns in patients with dark-skin types: the importance of case and assessor characteristics. Burns: journal of the International Society for Burn Injuries, 2015, 41(6): 1253-60.
10. Yu N, Yu Z, Pan Y A. Deep learning method for lincRNA detection using auto-encoder algorithm. BMC bioinformatics, 2017, 18: 511.
11. Liu X, Pan Z K, Li X Z, et al A review of deformable model methods in medical image segmentation technology. Computer application research, 2006, 23(008): 14-18.
12. Kho A, Zafar A, Tierney W. Information technology in PBRNs: the indiana university medical group research network (IUMG ResNet) experience. Journal of the American Board of Family Medicine, 2007, 20(2): 196-203.
13. Marsden M, Mcguinness K, Little S, et al. ResnetCrowd: A residual deep learning architecture for crowd counting, violent behaviour detection and crowd density level classification. IEEE, 2017.
14. Kelley C, Garson J, Aggarwal A, et al. Place prioritization for biodiversity reserve network design: a comparison of the SITES and ResNet software packages for coverage and efficiency. Diversity & Distributions, 2010, 8(5): 297-306.
15. Yun, Jiang, Li, et al. Breast cancer histopathological image classification using convolutional neural networks with small SE-ResNet module. Plos One, 2019.
16. Wu Z, Shen C, Hengel A V D. Wider or deeper: revisiting the resnet model for visual recognition. Pattern Recognition, 2016.
17. Iandola F, Moskewicz M, Karayev S, et al. DenseNet: Implementing efficient convnet descriptor pyramids. Eprint Arxiv, 2014.
18. Alphonse S, Abinaya S, Kumar N. Pain assessment from facial expression images utilizing Statistical Frei-Chen Mask (SFCM)-based features and DenseNet. Journal of Cloud Computing, 2024, 13(1).
19. Sen L, Rongguo Z, Dayang L, et al. Multimodal 3D DenseNet for IDH genotype prediction in gliomas. Genes, 2018, 9(8): 382.
20. Zhang Z, Liang X, Dong X, et al. A sparse-view CT reconstruction method based on combination of DenseNet and deconvolution. IEEE Transactions on Medical Imaging, 2018, 37(6): 1-1.
21. Shen F, Yang Y, Xiang Z, et al. Face identification with second-order pooling in single-layer networks. Neurocomputing, 2016, 187:11-18.
22. Nguyen D P, Huber P M, Metzger T A, et al. A specific mapping study using fluorescence sentinel lymph node detection in patients with intermediate- and high-risk prostate cancer undergoing extended pelvic lymph node dissection. European Urology, 2016, 70(5): 734~737.